Notes

CO_2-Induced Crystal Phase Transition from Form II to I in Isotactic Poly-1-butene

Lei Li, Tao Liu,* Ling Zhao,* and Wei-kang Yuan

State Key Laboratory of Chemical Engineering, East China University of Science and Technology, Shanghai 200237, P. R. China

Received November 12, 2008
Revised Manuscript Received January 20, 2009

Introduction

Isotactic poly-1-butene (iPB-1) is a polymorphous semicrystal polyolefin with many outstanding properties.[1−4] iPB-1 may exist in four different crystal structures, designated as forms I, II, III and I′.[5−10] Forms I and I′ have the same 3/1 helix conformation with twined hexagonal and untwined hexagonal crystal structure respectively.[11] Form II has the tetragonal unit cell packed by 11/3 helix conformation, and form III with 4/1 helix chain conformation has the orthorhombic unit cell.[12] Forms III and I′ are usually formed by crystallization from certain dilute solution.[13,14] Form I′ can also be obtained through crystallization from melt under high hydrostatic pressure.[15] Crystallized from melt under atmospheric pressure, form II can be obtained.[16] However, form II is unstable under ambient condition, and will transform into form I,[17−19] a stable crystal form. The transition of form II into I substantially enhances the mechanical, thermal and physical properties so that iPB-1 with form I is most widely used. However, completion of the transition under ambient condition requires several days or weeks. The slow transition rate has significantly limited the application of iPB-1. How to accelerate the phase transition has been studied by a number of methods such as application of uniaxial, shear orientation and hydrostatic pressure and addition of additives or other polymers.[4,20−29]

Supercritical carbon dioxide ($scCO_2$) has been increasingly considered and used as a promising alternative to organic and other toxic or harmful solvents for applications in polymer processing, such as grafting, foaming, and impregnation of additives.[30−33] On the one hand, the absorption of CO_2 in polymers can plasticize the materials and thus decrease the glass transition temperature and melting temperature.[34,35] On the other hand, the crystallization,[36−39] crystal form transformation[40,41] or conformational transition[42] may be induced by CO_2 treatment. In both cases, the structure and morphology of polymers have been changed significantly. To the authors' best knowledge, there is no report on the phase transition of crystal form II to I of iPB-1 induced by CO_2.

In this note, the effect of CO_2 on the crystalline transition of form II to I was investigated using high-pressure differential scanning calorimetry (DSC) and wide-angle X-ray diffraction (WAXD). In-situ high-pressure Fourier transform infrared spectroscopy (FTIR) was then used to detect the kinetics of the CO_2-induced phase transition from form II to I at different temperatures and pressures.

Experimental Section

Materials and Sample Preparations. iPB-1 pellets (PB 0110M) were supplied by Basell Polyolefins. Before used, they were purified by Soxhlet extraction in acetone for at least 24 h and then dried in a vacuum oven at 40 °C for 2 days. iPB-1 films with form II were prepared from pellets using a hot press at 170 °C and 10 MPa for 30 min and rapidly quenched by plunging into liquid nitrogen. The film thickness measured by micrometer caliper was 100 ± 20 μm. CO_2 (purity: 99.9% w/w) was purchased from Air Products Co., Shanghai, China.

CO_2 Treatments. Treatments of iPB-1 with form II using CO_2 were performed in a high-pressure vessel placed in a homemade oil bath with a temperature controller and its accuracy was ±0.5 °C.[33] The temperature of the oil bath was controlled at a desired temperature. The iPB-1 films with form II were placed in the vessel. The latter was then sealed and carefully washed with low-pressure CO_2. Thereafter the vessel was charged with a given amount of CO_2 using a syringe pump with an accuracy of 0.01 cm^3 (DZB-1A, Beijing Satellite Instrument Co., Beijing, China). The vessel was immersed in the oil bath and heated to the desired temperature. After a preset period of time, the vessel was cooled to the ambient temperature, and then the CO_2 was released.

Characterization of Polymers. DSC (NETZSCH DSC 204 HP, Germany) was used to characterize the melting behaviours of iPB-1 under ambient N_2 and high pressure CO_2. For each DSC measurement, about 5−10 mg of the iPB-1 was heated from 30 to 170 °C at a rate of 10 °C/min.[33] WAXD of the type Rigaku D/max 2550 VB/VC X-Ray Diffractometer (Cu Kα Ni-filtered radiation) was used to study the morphology of the iPB-1 samples. The scan rate was 1° (θ)/min and the diffraction angular range was between 3−50 ° 2θ. An in situ high-pressure FTIR of type Bruker Equinox-55 equipped with a Harrick high-pressure demountable liquid cell was used to study the kinetics of the phase transition from form II to I under CO_2, its details are described elsewhere.[42] FTIR spectra were recorded at a resolution of 4.0 cm^{-1} and a rate of 1 spectrum

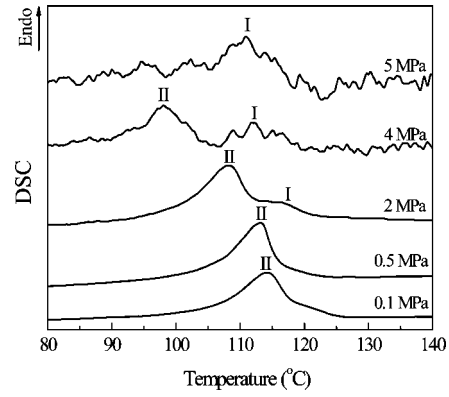

Figure 1. High-pressure DSC diagrams of the virgin iPB-1 with form II at different CO_2 pressures during the melting process.

* To whom correspondence should be addressed. Telephone: +86-21-64253175. Fax: +86-21-64253528. E-mail: (T.L.) liutao@ecust.edu.cn; (L.Z.) zhaoling@ecust.edu.cn.

10.1021/ma8025496 CCC: $40.75
Published on Web 02/18/2009

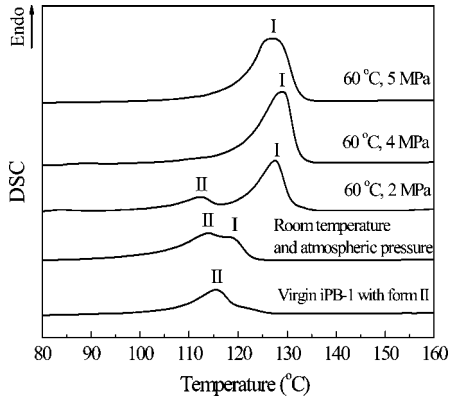

Figure 2. DSC curves of the virgin iPB-1 and that treated at different conditions under ambient N_2 atmosphere.

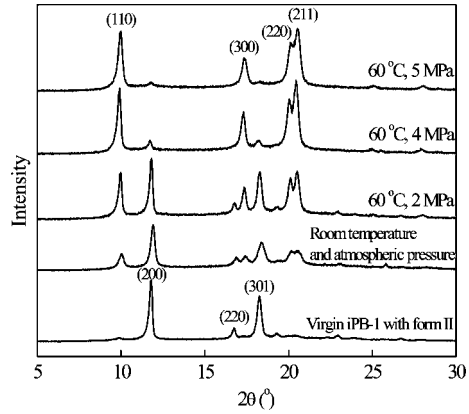

Figure 3. WAXD patterns of the virgin iPB-1 and that treated at different conditions.

per 32 s. The IR intensities refer to the peak height. The scanned wavenumber was in the range of 4000−400 cm^{-1}.

Results and Discussion

Melting Behavior of iPB-1 with Form II under CO_2. The melting behaviors of iPB-1 with crystal form II at different CO_2 pressures, characterized by DSC, are shown in Figure 1. The fluctuation in the DSC curves at 4 and 5 MPa was caused by the high pressure CO_2. At low CO_2 pressure, i.e. 0.1 or 0.5 MPa, the DSC thermogram shows a single endothermic peak which corresponds to the melting of form II. Moreover, the endothermic peak at 0.5 MPa shifts to the low-temperature side in comparison with that at 0.1 MPa, which might be due to plasticization of CO_2 on iPB-1. With increasing CO_2 pressure to 2 MPa, a second small endothermic peak develops on the high-temperature side of the main peak. This small endothermic peak was supposedly attributed to the melting of form I that was generated during the melting process under high pressure CO_2. Corresponding to 4 MPa, the second peak is more pronounced than that occurring at 2 MPa. When the CO_2 pressure was increased to 5 MPa, the endothermic peak of form II disappeared. That indicated that the form II transformed completely to the form I during the melting process under high pressure CO_2, and CO_2 substantially promoted the rate of the phase transition. It has been reported that that the form II of iPB-1 completely transformed to form I during the melting process under hydrostatic pressure higher than 90 MPa.[25] This work presented here showed the form II transformed into the form I completely during the melting process at a pressure of CO_2, as low as 5 MPa, and the pressurized CO_2 seemed to enhance the phase transition of form II to I more effectively than hydrostatic pressure.

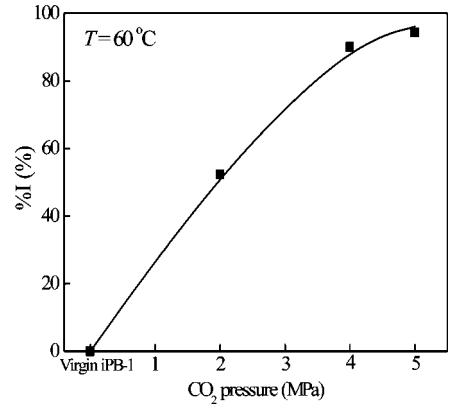

Figure 4. Content of form I in crystal phase of iPB-1 as a function of CO_2 treatment pressure at 60 °C for 8 h. The solid line only indicates the trend.

Effect of CO_2 on the Phase Transition of Form II to I. It has been reported that at atmospheric pressure, the phase transition rate of crystal form II to I was the fastest at room temperature and decreased abruptly at lower or higher temperatures.[6,21] To confirm the effect of CO_2 on increasing the transition rate of form II to I, the iPB-1 with form II was treated for 8 h at a relatively high temperature, i.e. 60 °C, and different CO_2 pressures, respectively. The iPB-1 with form II was also annealed for 8 h at room temperature and atmospheric pressure for comparison. After treatment, DSC and WAXD measurements were performed immediately under ambient N_2 atmosphere.

Figures 2 and 3 depict the DSC curves and WAXD patterns of the iPB-1 samples before and after treatments. In Figure 2, the virgin iPB-1 with form II presents only one endothermic peak around 116 °C in the DSC curve. A second small endothermic peak develops on the high-temperature side of the original peak in the DSC curve of the iPB-1 annealed at room temperature and atmospheric pressure. The second small endothermic peak might be attributed to the melting of form I that was generated under ambient condition. In the DSC curve of the iPB-1 treated at 60 °C and 2 MPa of CO_2, the area of the original endothermic peak significantly decreases and the second endotherm at the relatively high temperature of 127 °C increases.

Table 1. DSC and WAXD Results for iPB-1 before and after Treatments

treatment condition	T_{mII} (°C)	T_{mI} (°C)	ΔH_{II} (J/g)	ΔH_I (J/g)	α_{II} (%)	α_I (%)	α_{DSC} (%)	α_{WAXD} (%)
virgin	115.9		28.5		46.0	0	46.0	38.4
room temp and atmospheric pressure	113.9	118.7	22.7	14.9	36.1	10.6	46.7	39.5
60 °C, 2 MPa CO_2	112.9	127.9	10.4	40.3	16.7	28.6	45.3	37.3
60 °C, 4 MPa CO_2		128.9		65.4	0	46.4	46.4	40.2
60 °C, 5 MPa CO_2		126.9		65.8	0	46.7	46.7	41.7

T_{mII} and T_{mI} stand for the melting temperatures of forms II and I respectively, ΔH_{II} and ΔH_I for the melting enthalpies of forms II and I, α_{II} and α_I for the crystallinities of forms II and I, α_{DSC} for the total crystallinity obtained by the DSC measurement and α_{WAXD} for the total crystallinity determined by WAXD.

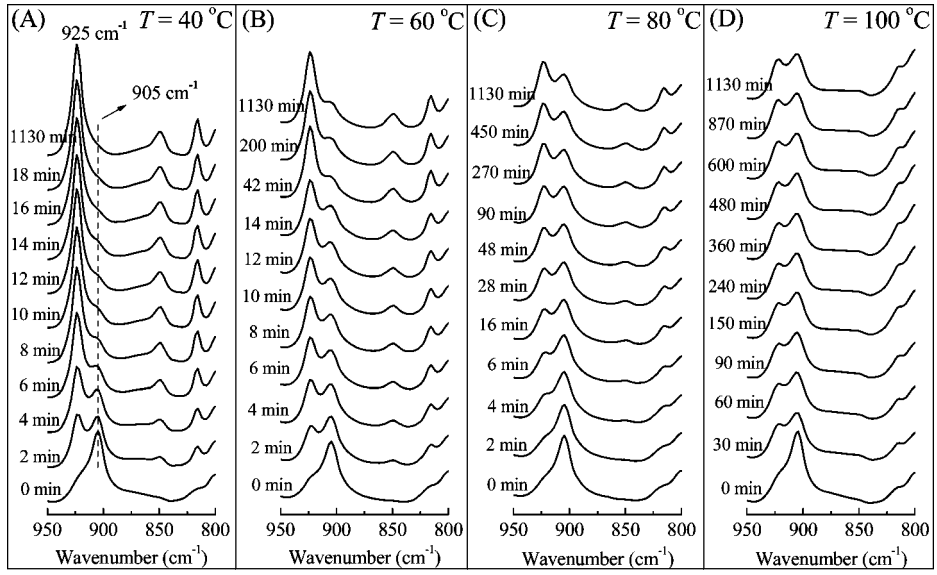

Figure 5. IR spectrum of iPB-1 with form II immersed in CO_2 at 4 MPa and various temperatures for different times.

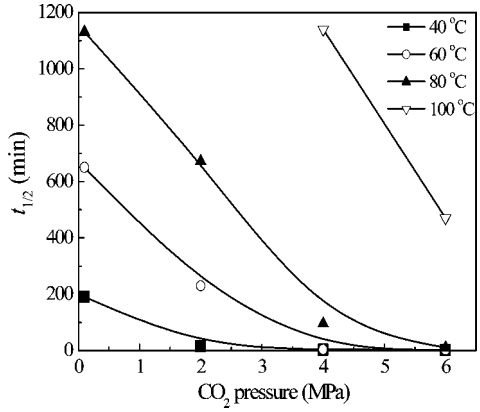

Figure 6. Effect of CO_2 pressure on $t_{1/2}$ at different temperatures. The solid lines only indicate the trends.

With further increasing CO_2 pressure, i.e., 4 and 5 MPa, the original endothermic peak disappeares and the area of the second endotherm peak increases. The WAXD pattern of the iPB-1 with form II exhibits three major peaks, at 11.9, 16.9, and 18.4°, corresponding to the diffraction of crystal reflections from planes (200), (220), and (301) respectively. However, the WAXD pattern of form I shows four major peaks, at 9.9, 17.3, 20.2, and 20.5°, corresponding to the diffraction of crystal reflections from planes (110), (300), (220), and (211), respectively.[43] As can be seen from Figure 3, the WAXD pattern of the virgin iPB-1 shows only form II existed, whereas that of the iPB-1 treated at 5 MPa of CO_2 shows only form I existed. In the other three iPB-1 samples, the WAXD patterns indicate both forms I and II coexisted. However, in comparison with the WAXD pattern of the iPB-1 annealed at room temperature and atmospheric pressure, the intensity of form I reflection in the CO_2-treated samples was significantly increased. With increasing the CO_2 pressure, the content of form II decreased while that of form I increased. The WAXD results verified that the endothermic peak in the virgin iPB-1 corresponded to the melting of form II, while the new one generated after CO_2 treatment corresponded to the melting of form I. Both DSC and WAXD measurements suggest that application of CO_2 was capable of promoting the phase transition of form II to I in iPB-1 even at a relatively high temperature.

Table 1 collects the melting temperatures and fusion enthalpies of the iPB-1 samples corresponding to the peaks and areas under the DSC curves in Fiugre 2. The heat fusion values of the two ideal infinite crystals are $\Delta H_{oII} = 62$ J/g and $\Delta H_{oI} = 141$ J/g for the crystal forms II and I, respectively.[44,45] The crystallinity of the iPB-1 samples for forms II and I was then calculated and given in Table 1. Although the crystallinity for form II decreased while that for form I increased with increasing the CO_2 treatment pressure, the total crystallinity of those samples measured by both the DSC and WAXD did not seem to change dramatically with the CO_2 treatment pressure, which is in good agreement with previous works.[44−47] This phenomenon might be related to different mobility of side-chain in form II and amorphous region. Miyoshi[48] studied the side-chain conformation and mobility in form II and amorphous region by solid-state ^{13}C NMR. It was pointed out that the side-chain conformation in form II was disordered as well as that in the amorphous region, but the side-chain mobility in form II was higher than that in the amorphous region. Therefore, the form II transformed to form I more easily than the amorphous region so that the transition from amorphous region to form I could be suppressed and the crystallinity remained unchanged. The relative percentage of crystal form I in the total crystal, % I, was calculated from the ratio $I_{9.9}/(I_{9.9} + I_{11.9})$, where $I_{9.9}$ and $I_{11.9}$ were the integral diffraction intensities of characteristic intense reflections of form I at 9.9° and that of form II at 11.9° in the WAXD patterns.[43] Figure 4 shows the %I as a function of the CO_2 treatment pressure at 60 °C for 8 h. With increasing the CO_2 treatment pressure, the content of form I initially increases and then it tends to level off. When the CO_2 pressure was up to 5 MPa, almost all form II transited into form I.

Kinetics of the CO_2-Induced Phase Transition from form II to I. Knowledge on the kinetics of CO_2-induced phase transition is helpful to reveal the phase transition mechanism. Previous work has shown there are distinct differences among the infrared spectrum range in 800−950 cm^{-1} between form II and I of iPB-1, and the bands at 905 and 925 cm^{-1} both correspond to the CH_2 and CH_3 rocking vibrations.[28] The band at 905 cm^{-1} is known to be the characteristic of form II while the one at 925 cm^{-1} is characteristic of form I.[49−51] Moreover, the bands at 905 and 925 cm^{-1} do not appear in the spectrum of pure CO_2.[42] Therefore, the infrared spectra might be used to

characterize the crystal phase transition of iPB-1 when the iPB-1 with form II was immersed into CO_2 in the high pressure IR cell. Figure 5 shows the spectra of iPB-1 with form II immersed in CO_2 at 4 MPa and various temperatures for different times. After CO_2 treatment at 40 °C for 18 min, the peak at 905 cm^{-1} disappeared, see Figure 5A, and the IR spectra tend to be the same as the one of iPB-1 treated for 1130 min, indicating completion of the phase transition. With increasing the temperature, the phase transition was obviously suppressed. As shown in Figure 5, parts B−D, the intensity of the band at 905 cm^{-1} for a given treatment time disappeared more slowly than that at 40 °C. The higher the temperature, the more slowly it disappeared. At 100 °C, even annealed for 1130 min, the intensity of the band at 905 cm^{-1} was still strong, indicating there was still a large content of form II in the iPB-1.

In a previous study, the absorbance ratio of the 905/925 cm^{-1} as a function of time was used to determine the rate of the crystal phase transition.[49] Following this approach, the transformed fraction of form I was derived from the ratio between the absorbance band area at 925 cm^{-1} (A_{925}) and the sum of that at 905 and 925 cm^{-1} ($A_{905} + A_{925}$). The superposition of two bands was analyzed by a PEAK-FIT V4.12 program that is usually applied to deconvolute complex IR spectra. The half-transition time, $t_{1/2}$, was obtained from the exponential curve of $A_{925}/(A_{905} + A_{925})$ as a function of treatment time. Figure 6 shows the effect of CO_2 pressure on the $t_{1/2}$ at different temperatures. At 100 °C and 0.1 and 2 MPa CO_2 pressure, the $t_{1/2}$ was too long to be observed so that it was not presented. At low CO_2 pressure, the $t_{1/2}$ at 80 or 100 °C was much longer than that at 40 or 60 °C. Danusso et al.[52] also pointed out that beyond 65 °C the phase transition of form II to I was never observed under atmosphere and the polymorph might be in a true metastable state. Figure 6 also shows that the $t_{1/2}$ significantly reduced with increasing the CO_2 pressure. Even at 60 and 80 °C, application of 6 MPa CO_2 reduced the $t_{1/2}$ to 2 and 10 min. It is well-known that addition of plasticizer, solid filler or other polymers can also promote the phase transition of form II to I. Schaffhauser[53] found a 3-fold increase in the phase transition rate of form II to I by incorporating 5 wt % of a plasticizer dioctylphthalate in iPB-1. Hong et al.[54] reported that sodium benzoate and polypropylene were effective nucleating agents in promoting the phase transition and the $t_{1/2}$ was shortened to several hours. Causin[4] showed that the addition of 5 wt % montnorillonite into iPB-1 reduced the $t_{1/2}$ from 11.5 to 2.2 h at room temperature and atmospheric pressure. In comparison with these reported data, CO_2 seems to play a much more substantial role on the phase transition than the plasticizer or additives used.

The transition of form II to I involves a change in the chain conformation and requires an elongation of the helix from 0.187 to 0.217 nm per chemical repeat unit.[4,55] It has been proposed[56−58] that normal stress and molecular mobility within noncrystalline regions play a crucial role in the phase transformation. In this work, it is specualted that the effect of CO_2 on the phase transition might result from the plasticization effect of CO_2 on the iPB-1. The absorbed CO_2 increased the free volume fraction of the polymer and promoted the motion of the polymer chain in the amorphous region. The extended chains in the amorphous region induced the tensile stress on the molecular parts that belonged to the crystalline lattice. The extra stress on the crystalline would cause the elongation of the chain helix and subsequently increase the phase transition rate. Direct validation of the speculation remains to be future work.

Conclusions

High-pressure DSC and WAXD measurements suggest that application of pressurized CO_2 was capable of promoting the phase transition of form II to I in iPB-1, which was much more effective in comparison with hydrostatic pressure. Detected by using the in situ high pressure FTIR, the kinetics of the CO_2-induced phase transition from form II to I indicated that the phase transition rate increased with increasing the CO_2 treatment pressure, while decreased with increasing the temperature. The mechanism of these observations will be investigated in future.

Acknowledgment. The authors are grateful to the National Science Foundation of China and PetroChina for the support of a joint project on multiscale methodologies (20490204), the National Science Foundation of China (50703011), Shanghai Rising-Star Program (08QA1402200), Shanghai Shuguang Project, Program for Changjiang Scholars and Innovative Research Team in University (IRT0721) and the 111 Project (B08021). Professor Zhibing Zhang, School of Chemical Engineering, The University of Birmingham, U.K., is thanked for making useful comments on the manuscript.

References and Notes

(1) Men, Y.; Rieger, J.; Homeyer, J. *Macromolecules* **2004**, *37*, 9481–9488.
(2) Fu, Q.; Heck, B.; Strobl, G.; Thomann, Y. *Macromolecules* **2001**, *34*, 2502–2511.
(3) Jiang, S.; Duan, Y.; Li, L.; Yan, D.; Chen, E.; Yan, S. *Polymer* **2004**, *45*, 6365–6374.
(4) Causin, V.; Marega, C.; Marigo, A.; Ferrara, G.; Idiyatullina, G.; Fantinel, F. *Polymer* **2006**, *47*, 4773–4780.
(5) Belfiore, L. A.; Schilling, F. C.; Tonelli, A. E.; Lovinger, A. J.; Bovey, F. A. *Macromolecules* **1984**, *17*, 2561–2565.
(6) Di Lorenzo, M. L.; Righetti, M. C. *Polymer* **2008**, *49*, 1323–1331.
(7) Kopp, S.; Wittmann, J. C.; Lotz, B. *J. Mater. Sci.* **1994**, *29*, 6159–6166.
(8) Maring, D.; Spiess, M. W. H. W.; Meurer, B.; Weill, G. *J. Polym. Sci., Part B: Polym. Phys.* **2000**, *38*, 2611–2624.
(9) Burns, J. R.; Turnbull, D. *J. Polym. Sci., Part A2: Polym. Phys.* **1968**, *6*, 775–782.
(10) Kaszonyiova, M.; Rybnikar, K.; Geil, P. H. *J. Macromol. Sci., Part B: Phys.* **2005**, *B44*, 377–396.
(11) Mathieu, C.; Stocker, W.; Thierry, A.; Wittmann, J. C.; Lotz, B. *Polymer* **2001**, *42*, 7033–7047.
(12) Miyoshi, T.; Hayashi, S.; Imashiro, F.; Kaito, A. *Macromolecules* **2002**, *35*, 2624–2632.
(13) Geacintov, C.; Schotl, R. S.; Miles, R. B. *J. Polym. Sci. Polym. Symp.* **1964**, *6*, 197–207.
(14) Kaszonyiova, M.; Rybnikar, F.; Geil, P. H. *J. Macromol. Sci., Part B: Phys.* **2004**, *B43*, 1095–1114.
(15) Nakamura, K.; Aoike, T.; Usaka, K.; Kanamoto, T. *Macromolecules* **1999**, *32*, 4975–4982.
(16) Warfield, R. W.; Petree, M. C. *J. Polym. Sci., Part A2: Polym. Phys.* **1967**, *5*, 791–794.
(17) Clampitt, B. H.; Hughes, R. H. *J. Polym. Sci. Polym. Symp.* **1964**, *6*, 43–51.
(18) Weynant, E.; Haudin, J. M.; G'Sell, C. *J. Mater. Sci.* **1980**, *15*, 2677–2692.
(19) Miller, R. L.; Holland, V. F. *J. Polym. Sci., Part B: Polym. Lett.* **1964**, *2*, 519–521.
(20) Samon, J. M.; Schultz, J. M.; Hsiao, B. S.; Wu, J.; Khot, S. *J. Polym. Sci., Part B: Polym. Phys.* **2000**, *38*, 1872–1882.
(21) Boor, J.; Mitchell, J. C. *J. Polym. Sci.* **1962**, *62*, S70−S73.
(22) Rubin, I. D. *J. Polym. Sci., Part A: Gen. Pap.* **1965**, *3*, 3803–3813.
(23) Arnon, S. *J. Appl. Polym. Sci.* **1982**, *27*, 1053–1065.
(24) Shieh, Y. T.; Lee, M. S.; Chen, S. A. *Polymer* **2001**, *42*, 4439–4448.
(25) Nakafuku, C.; Miyaki, T. *Polymer* **1983**, *24*, 141–148.
(26) Kishore, K.; Vasanthakumari, R.; Ramesh, T. G. *J. Polym. Sci., Part A: Polym. Chem.* **1986**, *24*, 2011–2019.
(27) Fujiwara, Y. *Polym. Bull.* **1985**, *13*, 253–258.
(28) Lee, K. H.; Snively, C. M.; Givens, S.; Chase, D. B.; Rabolt, J. F. *Macromolecules* **2007**, *40*, 2590–2595.
(29) Kalay, G.; Kalay, C. R. *J. Appl. Polym. Sci.* **2003**, *88*, 814–824.
(30) Li, B.; Hu, G.-H.; Cao, G.-P.; Liu, T.; Zhao, L.; Yuan, W.-K. *J. Appl. Polym. Sci.* **2006**, *102*, 3212–3220.
(31) Xu, Z.-M.; Jiang, X.-L.; Liu, T.; Hu, G.-H.; Zhao, L.; Zhu, Z.-N.; Yuan, W.-K. *J. Supercrit. Fluids* **2007**, *41*, 299–310.

(32) Tomasko, D. L.; Li, H. B.; Liu, D. H.; Han, X. M.; Wingert, M. J.; Lee, L. J.; Koelling, K. W. *Ind. Eng. Chem. Res.* **2003**, *42*, 6431–6456.
(33) Liu, T.; Hu, G. H.; Tong, G. S.; Zhao, L.; Cao, G. P.; Yuan, W. K. *Ind. Eng. Chem. Res.* **2005**, *44*, 4292–4299.
(34) Li, B.; Zhu, X.; Hu, G.-H.; Liu, T.; Cao, G.; Zhao, L.; Yuan, W. *Polym. Eng. Sci.* **2008**, *48*, 1608–1614.
(35) Yongli, M.; Sixun, Z. *Polymer* **1998**, *39*, 3709–3712.
(36) Zhai, W.; Yu, J.; Ma, W.; He, J. *Macromolecules* **2007**, *40*, 73–80.
(37) Liao, X.; Wang, J.; Li, G.; He, J. *J. Polym. Sci., Part B: Polym. Phys.* **2004**, *42*, 280–285.
(38) Mascia, L.; Del Re, G.; Ponti, P. P.; Bologna, S.; Di Giacomo, G.; Haworth, B. *Adv. Polym. Tech.* **2006**, *25*, 225–235.
(39) Gross, S. M.; Roberts, G. W.; Kiserow, D. J.; DeSimone, J. M. *Macromolecules* **2000**, *33*, 40–45.
(40) Ma, W. M.; Yu, J.; He, J. S. *Macromol. Rapid Commun.* **2005**, *26*, 112–115.
(41) Liao, X.; He, J.; Yu, J. *Polymer* **2005**, *46*, 5789–5796.
(42) Li, B.; Li, L.; Zhao, L.; Yuan, W. *Eur. Polym. J.* **2008**, *44*, 2619–2624.
(43) Luciani, L.; Seppala, J.; Lofgren, B. *Prog. Polym. Sci.* **1988**, *13*, 37–62.
(44) Azzurri, F.; Flores, A.; Alfonso, G. C.; Sics, I.; Hsiao, B. S.; Calleja, F. J. *Polymer* **2003**, *44*, 1641–1645.
(45) Alfonso, G. C.; Azzurri, F.; Castellano, M. *J. Therm. Anal. Calorim.* **2001**, *66*, 197–207.
(46) Rubin, I. D. *J. Polym. Sci., Part B: Polym. Lett.* **1964**, *2*, 747–749.
(47) Azzurri, F.; Flores, A.; Alfonso, G. C.; Calleja, F. J. B. *Macromolecules* **2002**, *35*, 9069–9073.
(48) Miyoshi, T.; Hayashi, S.; Imashiro, F.; Kaito, A. *Macromolecules* **2002**, *35*, 6060–6063.
(49) Luongo, J. P.; Salovey, R. *J. Polym. Sci., Part A2: Polym. Phys.* **1966**, *4*, 997–1008.
(50) Goldbach, G.; Peitscher, G. *J. Polym. Sci., Part B: Polym. Lett.* **1968**, *6*, 783–788.
(51) Luongo, J. P.; Salovey, R. *J. Polym. Sci., Part B: Polym. Lett.* **1965**, *3*, 513–515.
(52) Danusso, F.; Gianotti, G. *Angew. Makromol. Chem.* **1965**, *88*, 149–158.
(53) Schaffhauser, R. J. *J. Polym. Sci., Part B: Polym. Lett.* **1967**, *5*, 839–841.
(54) Hong, K.-B.; Spruiell, J. E. *J. Appl. Polym. Sci.* **1985**, *30*, 3163–3188.
(55) Marigo, A.; Marega, C.; Cecchin, G.; Collina, G.; Ferrara, G. *Eur. Polym. J.* **2000**, *36*, 131–136.
(56) Weynant, E.; Haudin, J. M.; G'Sell, C. *J. Mater. Sci.* **1982**, *17*, 1017–1035.
(57) Goldbach, G. *Angew. Makromol. Chem.* **1974**, *39*, 175–188.
(58) Goldbach, G. *Angew. Makromol. Chem.* **1973**, *29*, 213–227.

MA8025496